Structure Formation in Turbulent Plasmas[*)]

Sanae-I. ITOH

Research Institute for Applied Mechanics, Kyushu University, Kasuga 816-8580, Japan

This overview summarizes progress made to date on the Specially Promoted Research Project "Structure Formation and Selection Rule in Turbulent Plasmas." Keys for the progress of the project are a change of view, from one that is linear, local, and deterministic to one that is nonlinear, nonlocal, and statistical, and the integration of theory, simulation, and experiment.

1. Introduction

After five decades of studies of turbulence in plasmas [1], understanding of structure formation in turbulent plasmas has progressed substantially [2–5]. Recent developments in plasma physics, including fusion research in a new era of ITER as well as space research and astrophysics, have focused on structural formation in turbulent plasma associated with electromagnetic field formation [6]. Key to progress of the study of turbulent plasmas is a change of view, from one that is linear, local, and deterministic to one that is nonlinear, nonlocal, and statistical. Integration of theory, simulation, and experiment is another key to progress.

In this overview, we report progress made to date on the Specially Promoted Research Project "Structure Formation and Selection Rule in Turbulent Plasmas" [6, 7]. We first summarize the theory of microscopic turbulence, mesoscale fluctuations, and selection rules. We then explain direct computations using a global nonlinear simulation code, as well as describe the physics of mesoscale structures (such as zonal flow, zonal fields, and transport interface). Experimental tests on toroidal plasma experiments are also addressed. Finally, we report detailed experimental measurements, using a linear plasma device, of mesoscale structures (streamers and zonal flows) and nonlinear interactions among them. Confirmations by, and new challenges from, the experiments are stressed. This report focuses on the project results; detailed references of related work are given in review articles [8–12].

2. Theoretical Formulation and Simulations

In the study of structure formation and the selection rule, two fundamental issues exist in the theoretical framework, as shown in Fig. 1. First, a self-sustaining structure is realized by nonlinearity in plasma dynamics. Therefore, a nonlinear theory must be developed to describe the states far from thermodynamic equilibrium. Second, a statistical theory must be developed to calculate the transition probabilities between possible states. The theoretical framework has been extended to address these two requirements.

This procedure for developing a statistical theory for plasma turbulence is explained using the example of a reduced set of equations:

$$\frac{\partial}{\partial t}f + L^{(0)}f = N(f), \tag{1}$$

where $L^{(0)}$ is an operator for linear response, f is a fluctuation field such as $f^{\mathrm{T}} = (\phi, J, p)$, and $N(f)$ stands for nonlinear interactions. We adopt the following procedure:

(i) Decompose the nonlinear term into the coherent term $-\Gamma f$ and incoherent noise term R as

$$N(f) = -\Gamma f + R. \tag{2}$$

(ii) Solve a closed set of equations for coherent terms

$$(L^{(0)} + \Gamma)f = 0. \tag{3}$$

This gives self-consistent, self-sustained states. Multiple solutions are possible.

(iii) Analyze the effects of turbulent noise R on the mode (variable) of interest. Calculate the transition probability among nonlinear states, which are induced by the turbulent noise. From the transition probability, establish the selection rule for the nonlinear states.

We apply the dressed test mode method [2] and Mori's projection method [13] to the above system of equations to evaluate the memory function and random force [14]. This result gives a basis from statistical physics for the previously developed model, in which the method of dressed test mode was used. A summary is presented in Table 1.
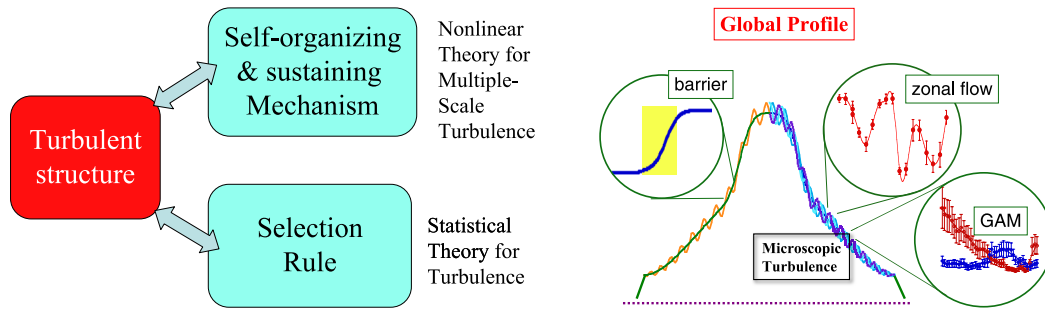
Fig. 1 (Left) Nonlinear, nonlocal, and statistical theory is necessary for the study of turbulent structure. (Right) Example of a multiplex turbulent structure in toroidal plasmas.

Table 1 Comparison of the result near thermodynamic equilibrium and that for far-from equilibrium.

	Near Thermodynamical Equilibrium	Far-Non-Equilibrium
Excitation		
(random)	Thermal excitation	Nonlinear drive
(coherent)	-	Instability drive
Balance	Fluctuation-Dissipation Theorem	Extended FD Theorem
Partition	Equi-partition $E_k \sim T\,k$ (2D)	Nonlinear Balance $E_k \sim \left\|\nabla p_0\right\| k^{-3}$
Min./Max. principle	Maximum Entropy/ Minimum entropy production rate	$S(\mathcal{E})$ minimum
Phase boundary	Maxwell's construction	$S(\mathcal{E}_A) = S(\mathcal{E}_B)$
Transition probability	$\ln(K) \sim -\Delta Q/T$ Arrhenius law	$K \propto \exp\left(-S(\mathcal{E}_{saddle})\right)$ Possible power law
Transport Matrix	Onsagar's symmetry	Not necessarily symmetric
Interference of fluxes	Curie's principle	Interferences between heat, particle and momentum
Transport coefficients	Independent of gradient	Depend on gradient

2.1 Transition probability and selection rule

Employing the coherent drag term and random noise, we derive the Langevin-type equation for the variable of interest, in the presence of background turbulence [15]. The variable X is the normalized variable of interest—for example, the normalized electric field $X = e\rho_p E_r/T$ in the study of H-mode transition. The dynamic equation for the variable X is given as

$$\frac{\partial}{\partial \tau}X + \Lambda X = w(\tau)g. \tag{4}$$

The probability density function (PDF) of X, $P(X)$, ensemble average, and transition probability are studied. The stationary solution of PDF $P_{eq}(X)$ is expressed as $P_{eq}(X) \propto g^{-1}\exp(-S(X))$ using the nonlinear potential $S(X) = \int^X 4\Lambda(X')g(X')^{-2}X'\mathrm{d}X'$. The minimum of $S(X)$ (apart from a correction $\ln g$)—that is, zero of Λ—predicts
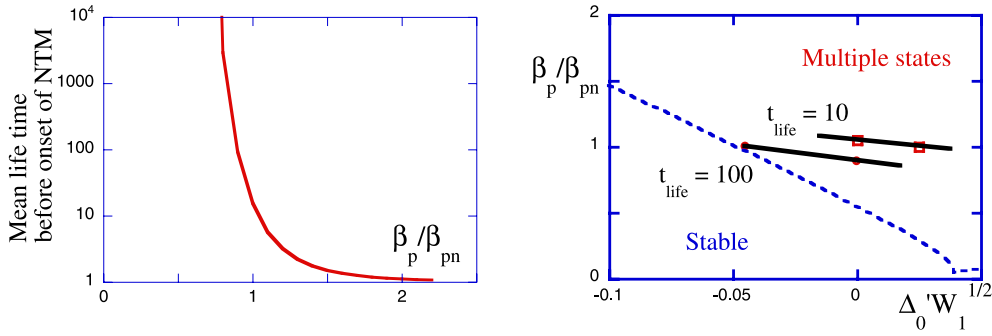
Fig. 2 (Left) Mean lifetime before onset of NTM as a function of plasma beta value (for $\Delta_0' = 0$). (Right) Contour of lifetime on the (Δ_0', β_p)-plane. Cusp for the multiple solutions is shown by the dotted line. Above the dotted line, multiple solutions are allowed and stochastic transition takes place. (See [16] for details of data.)

the probable state of X. Namely, $S(X)$ can have two minima at $X = X_L$ and $X = X_H$, which are separated by the local maximum at $X = X_m$. Bistable solutions $X = X_L$ and $X = X_H$ indicate hysteresis but the ensemble average $\langle X \rangle = \int X P_{eq}(X) dX$ changes smoothly as the global control parameter varies.

The transition probability is given as

$$r_{A \to B} = \frac{\sqrt{\Lambda_A \Lambda_m}}{2\pi} \exp(S(X_A) - S(X_m)), \qquad (5)$$

where $S(X) = \int^X 4\Lambda(X')g(X')^{-2}X'dX'$ is the nonlinear potential function, and the time rates $\Lambda_{A,m,B}$ are given as $\Lambda_{A,m,B} = 2X|\partial\Lambda/\partial X|$ at $X = X_{A,m,B}$.

2.2 Lifetime of plasma states near transition boundary

The transition probability gives the lifetime of a state, from which the plasma moves to the most probable state. The lifetime analysis is applied to the problem of the onset of neoclassical tearing mode. An explicit form of the lifetime is given as [16]

$$t_{life} = \frac{2\pi}{\eta \sqrt{\Lambda_0 \Lambda_m}} \exp(S(A_m)), \qquad (6a)$$

where A is the normalized amplitude of helical magnetic potential perturbation, and the nonlinear dissipation function is given as

$$S(A) = \Gamma_0 \frac{r_s^2}{\rho_b^2} \left(-\frac{4}{3}\Delta_0' A^{3/2} + hA^2 \right)$$
$$+ \Gamma_0 \frac{r_s^2}{\rho_b^2} \frac{\rho_b^2}{2r_s^2} \frac{L_q}{L_p} \frac{\beta_p}{\beta_{pn}} \ln\left(1 + \frac{r_s^4 A^2}{\rho_b^4}\right)$$
$$- \Gamma_0 \frac{r_s^2}{\rho_b^2} \frac{\beta_p}{\beta_{pn}} \left(A - \frac{w_{cut}^2}{r_s^2} \ln\left(1 + \frac{r_s^2}{w_{cut}^2}A\right) \right) \quad (6b)$$

with $\beta_{pn} = L_p/2a_{bs}\varepsilon^{1/2}L_q$ and

$$\Gamma_0 = \frac{2 \times 10^{-4}l}{k^3 \left(-\alpha^{-1/2}(1+\alpha) + s\sqrt{\beta m_i/m_e}\right)^2 s^4 R_M} \times \frac{r_s^6 \rho_b^2}{\delta^8}\alpha^{-11/2},$$

where δ is the collisionless skin depth, $\alpha = \varepsilon r_s \beta_p / L_p$ is the normalized pressure gradient for the case of current-diffusive ballooning mode turbulence, and other notations are given in [16]. The coefficient Γ_0 indicates the impact of the microscopic turbulence for the onset of the nonlinearly unstable mode.

The lifetime of the state $A = 0$, i.e., free from the neoclassical tearing mode (NTM), is shown in Fig. 2 (a). The unit of lifetime is $2\pi/\eta \sqrt{\Lambda_0 \Lambda_m}$, which is of the order of Rutherford growth time. The dependence of lifetime on plasma beta is shown. It is evident that lifetime strongly decreases as plasma beta increases. If plasma beta exceeds the effective phase limit β_{p*}, the lifetime value is on the order of magnetic diffusion time. The contour of the lifetime is shown in Fig. 2 (b).

Hysteresis for the onset of a magnetic island is also studied experimentally. The evidence of hysteresis and a comparison with experiments are given in [17].

2.3 Global nonlinear simulation

The theoretical study above indicates the importance of coupling between fluctuations with different scale lengths. With the development of global nonlinear simulations, the interactions between fluctuations with different scale lengths have been studied systematically [18–26]. A review of this work is published in [11]. Here, a prototypical example is presented.

It is shown explicitly, by employing the direct nonlinear simulations, that the novel mechanism of turbulence trigger is effective for neoclassical tearing mode in tokamaks. The nonlinear evolution of NTM in the presence of drift wave turbulence is investigated using the four-field neoclassical MHD equations, where fluctuating ion parallel flow and ion neoclassical viscosity are taken into account [18].

Nonlinear simulations with single helicity modes are performed using a spectral code. Figure 3 (a) shows the time evolution of electromagnetic energy for cases with different Fourier modes in the spectral space. It is found that nonlinear acceleration occurs in the early growing
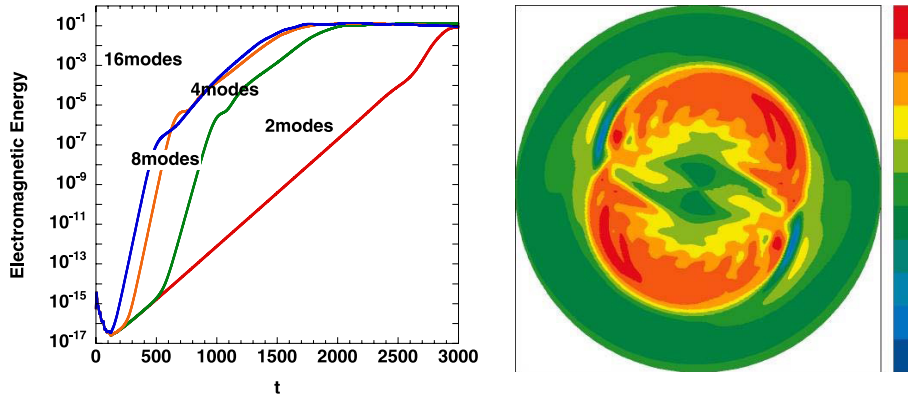
Fig. 3 (a) Time evolution of electromagnetic energy for various Fourier modes. (b) Contour of perturbation for multiple-scale turbulence. (See [18] for details.)

phase as the number of Fourier modes (n) increases. However, saturation amplitude is weakly affected by high-n modes. Acceleration of the growth of the tearing mode by background microscopic turbulence is clearly demonstrated. Figure 3 (b) shows the contour plot of perturbations, showing that the global magnetic island and microscopic turbulent fluctuations coexist.

Another important problem is the establishment of internal transport barriers. Selective turbulence spreading near the minimum of the safety factor was found to create an internal transport barrier [20]. The barrier forms in the region where linear instability exists, and the formation of barrier further increases the linear growth rate. This clearly demonstrates the nonlinear, nonlocal (multiplex and multiscale), and statistical nature of plasma turbulence.

3. Physics of Zonal Flow

Zonal flow in toroidal plasmas is, as a zero-th order description, constant flow on magnetic surface, independent of poloidal and toroidal angles, with its sign oscillating as the radius is increased. They are damped modes in linear theory but are driven by background microscopic turbulence induced by plasma inhomogeneities. The partition of energy from microscopic turbulence to linearly stable zonal flows thus reduces the level of microscopic fluctuations and turbulent transport.

The influence of zonal flows is central to the physics of confinement. Zonal flows are critically important in the design of fusion experimental reactors. In addition, zonal flows are prototypical examples of structure formation in nature. The study of zonal flows in laboratory plasma experiments has application in areas such as zonal flows and dynamo magnetic fields in solar and celestial plasmas.

Early work and advances in this area are surveyed in reviews [8, 9]. The essential elements in the physics of zonal flows are the following: (i) mechanism of zonal flows excitation; (ii) back interaction on turbulence; (iii) saturation mechanism of zonal flows; (iv) energy par-

tition between fluctuations and flows; and (v) turbulent transport coefficient dressed by zonal flows.

3.1 Mutual interactions and energy partition between fluctuations and flows

Nonlinear interactions between zonal flows and drift wave can be constructed for the zonal flow intensity V_Z^2 and total drift wave energy W as

$$\frac{\partial}{\partial t} W = \gamma_L W - \alpha V_Z^2 W - \Delta\omega_2 W^2 \qquad (7a)$$

and

$$\frac{\partial}{\partial t} V_Z^2 = \alpha W V_Z^2 - \gamma_{damp} V_Z^2 - \gamma_{NL}(V_Z^2) V_Z^2. \qquad (7b)$$

The term $\alpha W V_Z^2$ denotes the energy exchange where α is a coupling coefficient. The nonlinear damping rate of drift wave is expressed as $\Delta\omega = \Delta\omega_2 W$, and the term $\gamma_{NL}(V_Z^2)$ symbolically represents the self-nonlinear saturation mechanism of zonal flow.

The stationary state of drift waves and zonal flows, which follows Eq. (7), is dictated by $\alpha W V_Z^2$ and $\gamma_{NL}(V_Z^2) V_Z^2$. For the purpose of gaining analytic insight, let us choose a simple model of the form $\gamma_{NL}(V_Z^2) = \alpha_2 V_Z^2$. The stationary solution for Eq. (7) is given as either the solution without flow,

$$W = \frac{\gamma_L}{\Delta\omega_2} \qquad V_Z^2 = 0 \qquad (8a)$$

for the case of $\gamma_L < \gamma_{damp}\Delta\omega_2\alpha^{-1}$, or the solution with flow,

$$W = \frac{\gamma_{damp}\alpha + \alpha_2\gamma_L}{\alpha^2 + \Delta\omega_2\alpha_2} \qquad V_Z^2 = \frac{\gamma_L\alpha - \gamma_{damp}\Delta\omega_2}{\alpha^2 + \Delta\omega_2\alpha_2} \qquad (8b)$$

for the case of $\gamma_L > \gamma_{damp}\Delta\omega_2\alpha^{-1}$. When the driving source of drift waves is weak, zonal flow is not excited and bare fluctuations are realized. When the parameter exceeds the threshold, zonal flow is excited, and increment of fluctuation level becomes slower.

Equation (8) is relevant when the nonlinear decorrelation rate of drift waves is large. When the drift wave amplitude is low and $\Delta\omega_k$ is small, special care is necessary. A famous example is the Dimits shift problem [27]. In such a case, zonal flow saturates when trapping becomes effective—that is, $\Delta\omega_k = \omega_{\text{bounce}} \propto \sqrt{V_Z}$. Using the renormalized growth rate of zonal flow, the saturation condition for zonal flow in the absence of collisional damping is derived as [28]

$$\Delta\omega_k^2 = Ck_\theta^2\rho_s^2 U^2 - \omega_{\text{bounce}}^2, \tag{9}$$

where $C \sim 2$ is a numerical coefficient of order unity. Note the relationship $\omega_{\text{bounce}}^2 \propto \omega_k U$.

Figure 4 shows the energy partition between flow and fluctuations in the absence of collisional damping. Even in the absence of fluctuations, zonal flows can have finite amplitude.

3.2 Turbulent transport coefficient dressed by zonal flow

When the damping rate of zonal flow is large, the turbulent transport coefficient is determined by bare microscopic fluctuations. When fluctuations are driven by linear instability, thermal diffusivity is given as

$$\chi_i = \frac{\gamma_L}{k_r^2}. \tag{10a}$$

When zonal flows are excited but weak so that $\gamma_{\text{NL}}(V_Z^2) < \gamma_{\text{damp}}$ holds,

$$\chi_i \sim \sqrt{\frac{\gamma_{\text{damp}}}{\alpha}}\frac{\omega_*}{k_r^2}, \tag{10b}$$
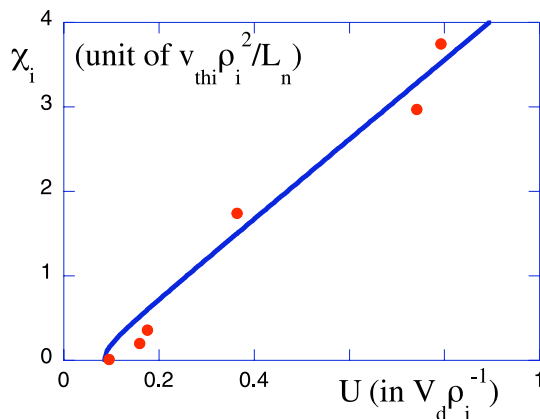

Fig. 4 Comparison of the relationship $\chi_i(U)$ for the steady state of ion-temperature-gradient mode [28]. Zonal flow vorticity is in units of $V_d\rho_i^{-1}$ and thermal conductivity is in units of $v_{\text{thi}}\rho_i^2 L_n^{-1}$. Theory (solid line) and DNS data (dots) quoted from [29].

which is independent of γ_L. In the limit of large γ_L, thermal diffusivity is given as

$$\chi_{\text{III}} = \frac{Ck_\theta^2\rho_s^2\omega_*}{2\alpha}\left(-1 + \sqrt{1 + \frac{4\alpha}{Ck_\theta^2\rho_s^2\omega_*^2}(\gamma_L - \gamma_{\text{L,c}})}\right)\frac{\omega_*}{k_r^2}, \tag{10c}$$

where the boundary $\gamma_{\text{L,c}}$ is given as $\gamma_{\text{L,c}}/\omega_* = 2\sqrt{2}C^{-1}q_r^2 k_\perp^{-2}$. Thus, the coefficient of turbulent transport, which is dressed by zonal flow, is obtained.

4. Experimental Studies on Zonal Flow and Zonal Fields

Stimulating developments have been made in experimental studies of zonal flow and geodesic acoustic modes (GAMs). Experimental discovery of zonal flow is reported in [30]. Articles in cluster papers [10] and in reviews [8, 12], for example, describe rapid progress in this field of research. Contributions have been given from various experiments, including toroidal systems as well as linear devices, in alphabetical order, ASDEX-U, CASTOR, CHS, CLM, CSDX, DIII-D, H1-heliac, HL-2A, HT-6M, HT-7, JFT-2M, JIPPT-IIU, T-10, TEXTOR, TEXT-U, TJ-II, and TJ-K. These are summarized in Table 1 of [12], and further reports on LMD-U are found in [6].

4.1 Identification of zonal flow and GAMs

The most important progress has been the experimental discovery of zonal flow, which was made in a compact helical system (CHS) device. The radial electric field is measured in the device at two different toroidal angles. The power spectrum of electric field fluctuation is shown in Fig. 5 (left) with cross correlation between electric fields at two different locations. Strong correlation in the low-frequency regime indicates zonal flow. Two-point and two-time correlations of low-frequency components of the electric field are shown in Fig. 5 (right). The reference radius is chosen as $r = 12$ cm, and the radius of the other observation point is varied. The zonal flow has a radial wavelength of a few centimeters and an autocorrelation time of a few milliseconds. These are longer than those for microscopic fluctuations, confirming that zonal flows is mesoscopic.

Many researchers have reported observations of GAM oscillations in toroidal plasmas and compared observed peaks with expected GAM frequencies. Figure 6 is reproduced from [12]. The frequency of GAMs is now widely validated.

The radial structure of GAMs has also been investigated. The JFT-2M group has reported observation of GAM eigenmode characteristics. In addition, outward propagation characteristics of GAMs have been deduced [31]. Theories show that GAMs have eigenmode structure owing to temperature inhomogeneity and can propagate in a radial direction [32,33]. GAM spectroscopy has been proposed to measure ion density [34].
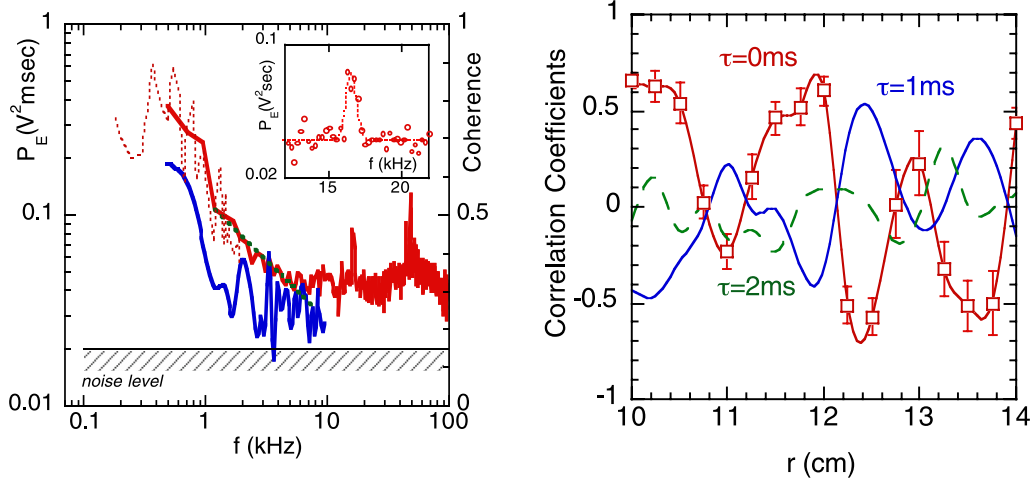
Fig. 5   (Left) Spatiotemporal structure of stationary zonal flows evaluated from the correlation function in a CHS device. (Right) Spatial correlation with time lag of $\tau = 0$, 1, and 2 ms. The reference radius is chosen at $r = 12$ cm [12, 30].
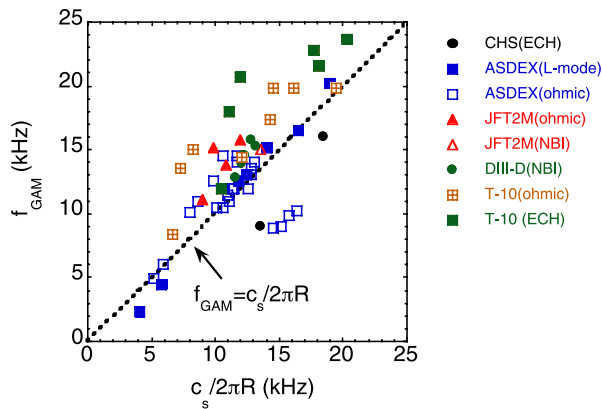

Fig. 6   Comparison between observed GAM frequency and theoretical prediction. c_s is the ion sound velocity; R is the major radius. (Quoted from [12].)

4.2   Nonlinear interactions among zonal flow and fluctuations

Identification of zonal flow requires measurement of nonlinear coupling between zonal flow and fluctuations. A systematic study using bicoherence analysis has been developed on coupling between GAMs and drift waves [35–41]. Figure 7 shows bicoherence analysis for the edge fluctuation of JFT-2M plasma. The component with the local GAM frequency has an unambiguous squared bicoherence for $\omega_1 + \omega_2 = \omega_{GAMs}$, which verifies coupling with broadband microscopic fluctuations (in the range >30 kHz). We observe that any pair of drift wave modes interacts with a common GAM component, so that the biphase takes almost constant values. In contrast, for combinations of three drfit wave modes, the biphase randomly changes by choice of interacting pair. The bicoherence and biphase were compared with theoretical prediction [42] in the article [39]. The observed bicoherence is within the order of

magnitude of theoretical prediction, providing quantitative confirmation that GAMs have been observed.

As is explained in the theory of zonal flow growth based on modulational instability, excitation of zonal flow is accompanied by envelope modulation of background microfluctuations [8]. Such modulation was also observed [36, 43].

Fluctuation-driven Reynolds stress is an essential issue in the physics of zonal flow, and it has been measured using various devices. Reports of semi-quantitative agreement [44] show that turbulence-driven stress is the dominant source that drives global plasma flow shear in linear plasma.

4.3   Suppression of turbulent transport by zonal flow

Measurements of the effects of zonal flow on turbulent transport have been made using CHS device [45–48]. Particle flux is given as $\Gamma = \sum_{\omega} \Gamma_\omega$, $\Gamma_\omega = \frac{1}{B}\langle \tilde{E}_\omega \tilde{n}_\omega \cos \alpha_\omega \rangle$, where $\tilde{E}_\omega$ is electric field perturbation, $\tilde{n}_\omega$ is density perturbation, and α_ω is phase difference. Γ_ω is high at the bottom of the zonal flow potential (where the zonal flow electric field is opposite to the mean dc radial electric field) and low at the peak of the zonal flow potential (Fig. 8). This observation is consistent with theoretical modeling, which predicts that fluctuations tend to accumulate in the trough of zonal flows.

4.4   Control of transport by modifying the damping rate of zonal flow

Turbulent transport is strongly influenced by the damping rate of zonal flow [8]. This introduces the idea of controlling turbulent transport by modifying the damping rate of zonal flow. This working hypothesis was tested in the analysis of CHS plasma. It is known that electron
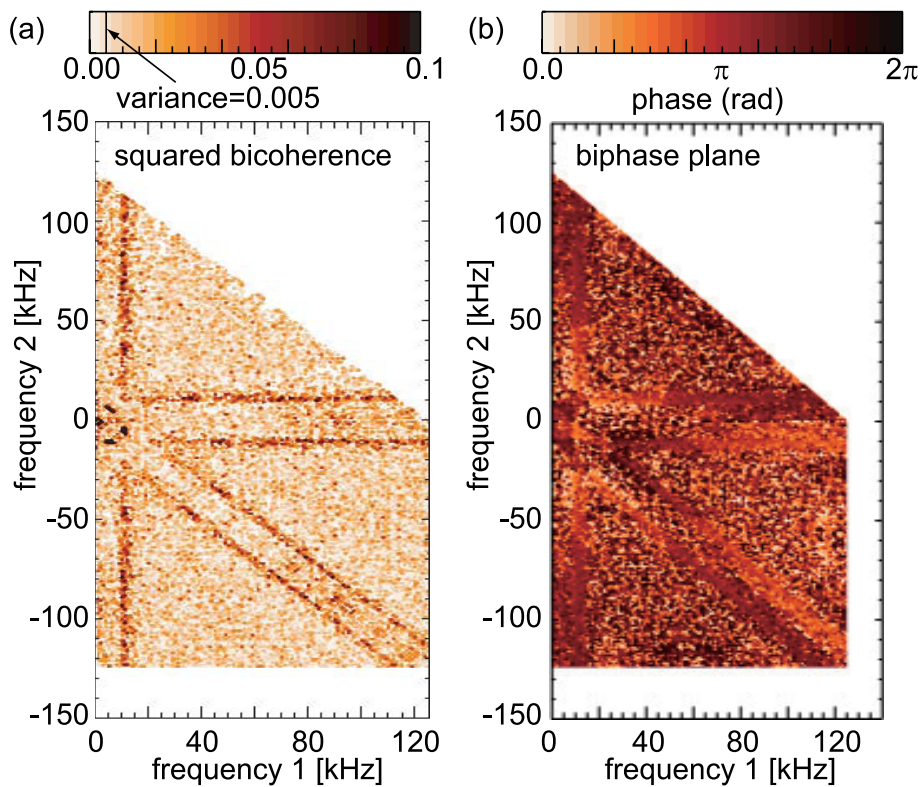
Fig. 7 Bicoherence analysis to show coupling between GAM and background turbulence in JFT-2M (see [36] for details). (a) Bicoherence evaluated with potential fluctuation at the plasma edge. (b) Corresponding biphase.
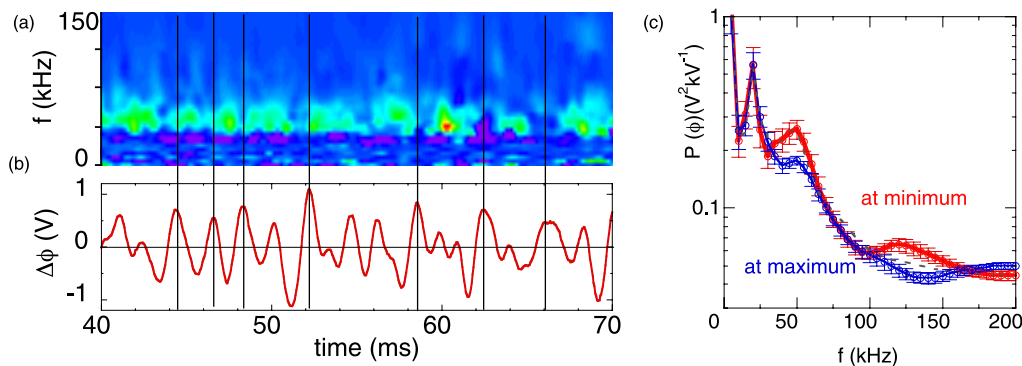

Fig. 8 Modulation effect of stationary zonal flow on particle transport in a CHS device [45]. (a) Temporal evolution of stationary zonal flows. (b) Image plot of particle flux. (c) Conditional averages of potential fluctuation spectra in the time windows discriminated by the phase of zonal flow—that is, maxima, zero, and minima.

turbulent transport is reduced in the plasma core, where the electric field itself is high but its shear is insufficient to suppress turbulence (see a review in [49]). The role of zonal flow in the formation of an internal transport barrier in toroidal helical plasma has been analyzed [50]. Reduction of turbulent transport in the core of e-ITB plasma, via enhanced zonal flow, has been experimentally confirmed, as shown in Fig. 9. It is clearly demonstrated, theoretically and experimentally, that the damping rate of zonal flow governs the global confinement of toroidal plasmas.

4.5 Zonal fields

The electromagnetic counterpart of zonal flow is a zonal field [8]. Zonal fields can influence the current profile or stability of tokamaks. In addition, zonal fields are considered to be mesoscale dynamos. Thus, we have a unique opportunity to study the physics of dynamo magnetic fields [51] by laboratory measurement of the process whereby structured magnetic fields are generated by microscopic turbulence. Experimental evidence for zonal fields has recently been reported [52]. Zonal fields that are in the poloidal direction and change sign with radial wave-
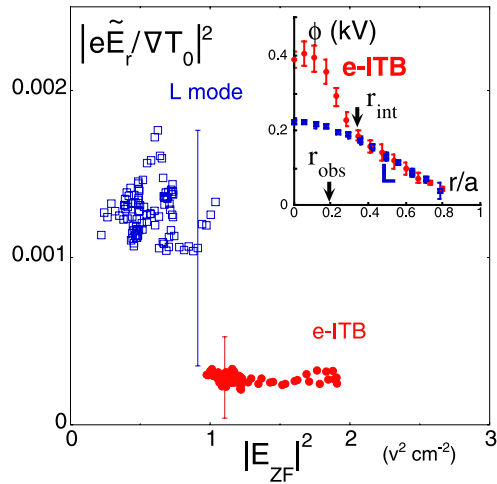
Fig. 9 Simultaneously observed zonal flows and microturbulence intensities during the e-ITB phase (solid circle, red) and L-phase (open circle, blue). Vertical and horizontal axes are normalized fluctuation amplitude $|e\tilde{E}_r/\nabla T_0|^2$ and zonal flows amplitude $|E_{ZF}|^2$, respectively. The insert shows the profile of mean potential for e-ITB and L plasmas. Locations of interface and observation, r_{int} and r_{obs}, are also indicated [50].

length of a few centimeters were discovered in CHS plasmas using a dual heavy-ion beam probe system. Details of the experimental study of zonal fields are found in [53–55].

5. Experimental Study of Drift Wave Turbulence in Linear Plasmas

In the Specially Promoted Research Project "Structure Formation and Selection Rule in Turbulent Plasmas," particular focus is placed on use of the linear plasma device LMD-U. A unification of the methods of research—that is, theory, simulation, and experiments—is pursued in the project. For this purpose, the LMD-U device has been upgraded at Kyushu University [56], and a numerical linear device (NLD) has also been developed [57]. Detailed measurements of turbulent fields, combined with predictive studies by NLD, have enabled the study of nonlinear interactions in drift wave turbulence. Extensive research has been performed worldwide on plasma turbulence in linear plasma devices (see references in [44, 56]). These studies propelled research trends in this direction. In addition, the discovery of streamers followed [58]. Here, these results are briefly reported.

5.1 LMD-U device and study of drift wave turbulence

LMD-U linear plasma has a cylindrical shape with a diameter of about 100 mm and an axial (z) length of 3740 mm. Under the experimental conditions of 3 kW of 7 MHz rf power, 0.01-0.15 T of axial magnetic field (in the $+z$ direction), and 1-6 mTorr of argon pressure in the

source region, the electron density and temperature of the plasma were found to be about 10^{19} m^{-3} and 3 eV, respectively. The electron density gradient is steep in the radius range $r = 30$-40 mm and produces resistive drift wave instabilities propagating in the poloidal direction. Drift waves and route to drift wave turbulence have been observed in this plasma [59]. With a 64-channel poloidal Langmuir probe array, which is able to measure the precise poloidal wave numbers of the fluctuations [60], two-dimensional (poloidal wave number k_θ and frequency ω) power spectra of the drift wave turbulence were observed. A number of fluctuation peaks and broadband components appear in the two-dimensional power spectrum [61]. Ion flow velocity near the end plate has been measured [62]. Pumps have been designed to suppress neutral density, following the simulation of neutral particles [63].

Increasing the magnetic field and/or decreasing the argon pressure causes turbulent fluctuations. Figure 10 (left) shows spatiotemporal fluctuations of the ion saturation current measured with the 64-channel probe array. The waveform shows that the plasma is in a turbulent regime. There is a main $m = 1$ fluctuation in the electron diamagnetic direction together with multiplex structures separating and combining. Figure 10 (right) shows the two-dimensional power spectrum $S(m, f)$. The spectrum shows a number of fluctuation peaks in m–f space. Some of the peaks satisfy the linear dispersion relationship calculated in [57]. The fluctuation peaks do not satisfy a single proportional relationship between m and f. Therefore, many of the peaks are excited by nonlinear couplings with other peaks. In addition, there are broadband fluctuation components other than the fluctuation peaks.

Nonlinear couplings in the turbulent regime are confirmed by bispectral analysis [58, 64]. It was found that three primary modes induce other peaks in sequence.

5.2 Discovery of streamers

Theory predicts that drift waves can cause self-focusing in the direction of propagation (with small modification in radial direction), called a "streamer" [8, 65]. This self-organization of turbulence is complementary to zonal flow, which is constant in the poloidal direction. Numerical linear device (NLD) predicts that a streamer occurs when the damping rate of zonal flow is large in a linear plasma device [66].

We have identified the streamer structure—that is, the bunching of drift waves—for the first time, confirming nonlinear interactions. Figure 11 shows the emergence of a streamer. Thin stripes (fast propagation in poloidal direction) denote waves, and their envelope is focused in the θ-direction. The peaks and troughs of the envelope propagate slowly in the poloidal direction. The time scale of propagation of the envelope in the laboratory is about few-to-ten times larger than that of waves. Taking into account plasma rotation introduced in the analysis of wave disper-
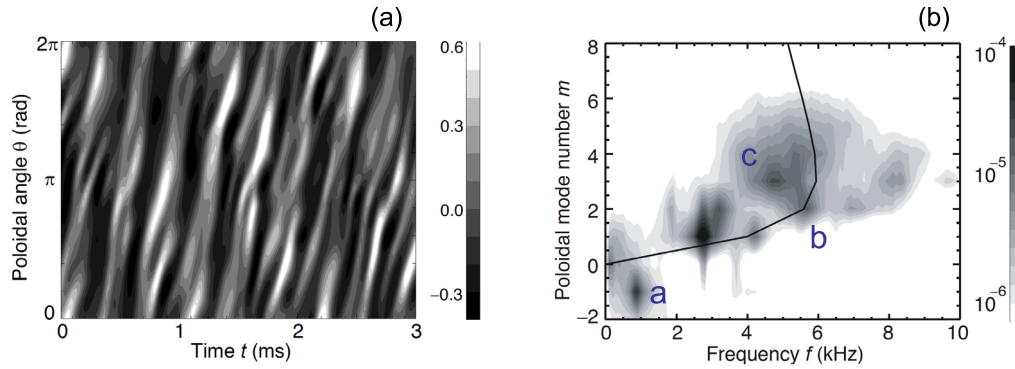
Fig. 10 (Left) Spatiotemporal behaviors of ion-saturation current fluctuations (arbitrary unit) measured with 64-channel poloidal probe array. Discharge conditions (magnetic field, argon pressure) are (0.09 T, 2 mTorr). (Right) Contour plots of two-dimensional power spectrum $S(m, f)$ (arbitrary unit). Solid line shows linear dispersion relationship of drift waves calculated by numerical code analyses. (Reproduced from [56].)
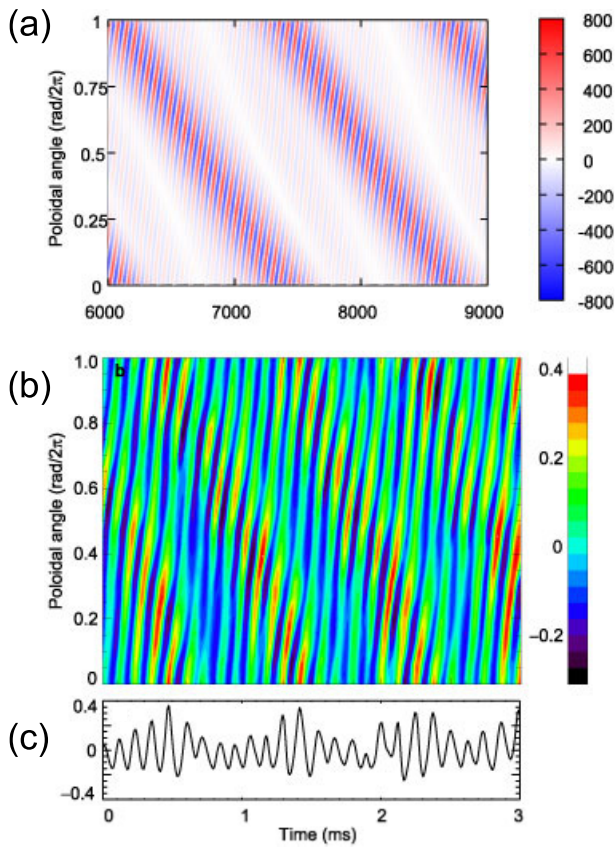

Fig. 11 Streamer in a linear plasma device. Prediction by simulation (top) and measurement (middle and bottom). Simultaneous measurement of the spatiotemporal behaviors of ion-saturation current fluctuations is given on the surface, $r = 4$ cm and $z = 1.885$ m. Temporal behavior at $\theta = 0$ shows bunching of the wave (bottom). (Reproduced from [58].)
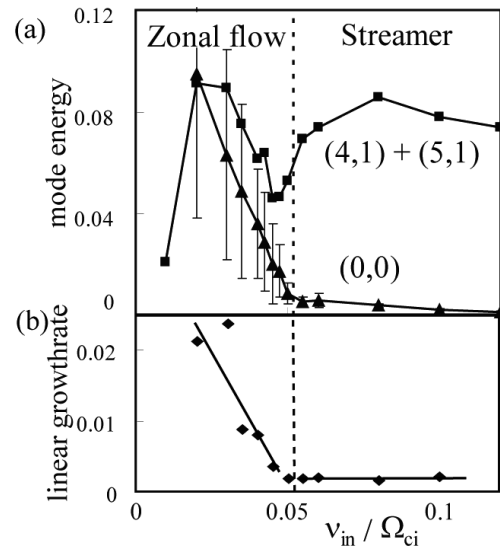

Fig. 12 Dependencies of (a) fluctuation energies of the electrostatic potential and (b) instantaneous linear growth rate of $(4, 1)$ mode on the neutral density. Result is obtained using a numerical linear device [71].

Fig. 10 (right). The peak (X) is, for example, (2c), (b + c), etc. Nonlinear coupling of (a) with other quasimodes having $m \geq 2$ is confirmed. The streamer structure was shown to be extended in the radial direction using two poloidal probe arrays as well as a two-dimensional movable probe. The nonlinear triplet coupling that leads to streamer formation lasts longer than the autocorrelation time of fluctuations. Thus, we have experimentally quantified that nonlinear coupling determines multiple characteristic timescales in turbulent plasmas. The density and potential fluctuation structures in LMD-U are reported in [67].

5.3 Zonal flow in a linear plasma device

Zonal flow is also studied in the linear plasma LMD [68–70]. Drift waves and low-frequency zonal

sion, the rotation frequency of the envelope in the plasma frame reduces to O (100 Hz). This modulation of envelope is created by nonlinear coupling of many fluctuation components with $m \geq 2$, such as peaks (X) and (X ± a) in

flow coexist. Two distinctive modes at frequencies 0.3-0.5 kHz (zonal flow) and 6-8 kHz (drift wave) are observed. The zonal flow is located at $r < 4.5$ cm, associated with poloidal velocity fluctuations. The drift wave has maximal amplitude in the steep density gradient region, $m/n = 3\text{-}5/2\text{-}3$, and finite radial wave numbers.

The radial wave number profile of the zonal flows has a shear structure at the radial location where the drift wave has maximal normalized fluctuation amplitude. The radial wave number profile of the drift wave shows vortex tilting, resulting in generation of stationary turbulence Reynolds stress gradient per mass density. Envelope and bispectral analyses detect significant nonlinear interactions between zonal flows and drift waves and confirm nonlinear interaction between them. Energy exchange between waves and flow is also confirmed.

Figure 12 shows the selection rule between zonal flow and a streamer [66, 71].

6. Summary

We report herein progress in the project "Structure Formation and Selection Rule in Turbulent Plasmas." In this focused study, we have developed a new view of plasma turbulence as being nonlinear, nonlocal, and statistical. This replaces the previous view of it being linear, local, and deterministic. Because the previous view assumed linear growth in a local model, it gave only a limited view of the properties of plasma [72]. Progress has been made in the nonlinear statistical theory of turbulence, global simulations, and methods of nonlinear data analysis. By these new methodologies, we have clarified our understanding of structure formation and transition, phase boundaries, transition probabilities, and state lifetimes. Global simulation demonstrates that dynamic behavior as well as barrier formation is influenced by the presence of multiple-scale turbulence. The physics of zonal flows is also developed, and the experimental discovery of zonal flows, zonal fields, and streamers is made. Nonlinear interactions between mesoscale structures and microscopic turbulence have also been verified unambiguously. This project thus successfully unified the research methods of theory, simulation, and experiment in the study of turbulent plasmas.

This research is expected to be extended in various directions. One direction is to investigate plasmas in nature. Initial efforts have investigated the dynamo magnetic field, solar tachocline, magnetic and velocity structures, and more [73–75]. Another direction is to investigate plasmas in the laboratory by studying phenomena such as transit transport, in which change propagates across the plasma column much faster than would be the case from diffusion. Such phenomena have been observed in toroidal plasma experiments [76–81]. Studies have been initiated of long-range interactions [8,82], dynamic competition among various modes [83–85], and two-dimensional structure formation [86–91]. The study of dynamical response of turbu-

lence will be systematically pursued in the Project "Integrated Research on Dynamic Response and Transport in Turbulent Plasmas."

[1] B.B. Kadomtsev, *Plasma Turbulence* (Academic Press, New York, 1965); R.D. Sagdeev and A.A. Gareev, *Nonlinear Plasma Theory* (Benjamin, New York, 1969); R. Balescu, *Aspects of Anomalous Transport in Plasmas* (IoP, Bristol, 2005).

[2] K. Itoh, S.-I. Itoh and A. Fukuyama, *Transport and Structural Formation in Plasmas* (IoP, London, 1999).

[3] S.-I. Itoh and N. Kawai, *Bifurcation Phenomena in Plasmas* (Kyushu Univ., Fukuoka, 2002).

[4] A. Yoshizawa, S.-I. Itoh and K. Itoh, *Plasma and Fluid Turbulence* (IoP, England, 2002).

[5] S.-I. Itoh and K. Itoh, Plasma Phys. Control. Fusion **43**, 1055 (2001).

[6] S.-I. Itoh, J. Plasma Fusion Res. **83**, 241 (2007).

[7] S.-I. Itoh, J. Plasma Fusion Res. **81**, 212 (2005).

[8] P.H. Diamond, S.-I. Itoh, K. Itoh and T.S. Hahm, Plasma Phys. Control. Fusion **47**, R35 (2005).

[9] K. Itoh, S.-I. Itoh, P.H. Diamond, T.S. Hahm, A. Fujisawa, G.R. Tynan, M. Yagi and Y. Nagashima, Phys. Plasmas **13**, No. 5, 055502 (2006).

[10] S.-I. Itoh, ed., Cluster papers in Plasma Phys. Control. Fusion **48**, No.4 (2006).

[11] M. Yagi, S.-I. Itoh, K. Itoh and P.H. Diamond, Contrib. Plasma Phys. **48**, 13 (2008).

[12] A. Fujisawa *et al.*, Nucl. Fusion **47**, S718 (2007).

[13] H. Mori, Prog. Theor. Phys. **33**, 423 (1965).

[14] S.-I. Itoh, K. Itoh and H. Mori, J. Phys. Soc. Jpn. **75**, No.3, 034501 (2006).

[15] F. Spineanu, M. Vlad, K. Itoh and S.-I. Itoh, Review of analytical treatments of the barrier-type problems in plasma theory, in *Trends in Chemical Physics Research* (NOVA Science Publisher, 2006).

[16] S.-I. Itoh, K. Itoh and M. Yagi, J. Phys. Soc. Jpn. **74**, 947 (2005).

[17] K. Ida, S. Inagaki, M. Yoshinuma, Y. Narushima, K. Itoh *et al.*, Phys. Rev. Lett. **100**, 045003 (2008).

[18] M. Yagi *et al.*, Proc. of 20th Fusion Energy Conf. 2004, TH/P5-17.

[19] M. Yagi, S. Yoshida, S.-I. Itoh, H. Naitou, H. Nagahara, J.-N. Leboeuf, K. Itoh, T. Matsumoto, S. Tokuda and M. Azumi, Nucl. Fusion **45**, No.7, 900 (2005).

[20] M. Yagi, T. Ueda, S.-I. Itoh, M. Azumi, K. Itoh, P.H. Diamond and T.S. Hahm, Plasma Phys. Control. Fusion **48**,

A409 (2006).

[21] M. Honda and A. Fukuyama, Nucl. Fusion **46**, No.5, 580 (2006).

[22] M. Yagi, S.-I. Itoh, K. Itoh, M. Azumi, P.H. Diamond, A. Fukuyama and T. Hayashi, Plasma Fusion Res. **2**, 025 (2007).

[23] S. Nishimura, M. Yagi, S.-I. Itoh, M. Azumi and K. Itoh, J. Phys. Soc. Jpn. **76**, 064501 (2007).

[24] A. Smolyakov, P.H. Diamond, M. Yagi, K. Itoh and S.-I. Itoh, J. Phys. Soc. Jpn. **76**, 113501-1 (2007).

[25] S. Nishimura, M. Yagi, S.-I. Itoh, M. Azumi and K. Itoh, J. Phys. Soc. Jpn. **77**, 014501 (2008).

[26] S. Sugita, M. Yagi, S.-I. Itoh and K. Itoh, Plasma Fusion Res. **3**, 040 (2008).

[27] A. Dimits *et al.*, Phys. Plasmas **7**, 969 (2000).

[28] K. Itoh, K. Hallatschek, S.-I. Itoh, P.H. Diamond and S. Toda, Phys. Plasmas **12**, 062303 (2005).

[29] K. Hallatschek, Phys. Rev. Lett. **93**, 065001 (2004).

[30] A. Fujisawa *et al.*, Phys. Rev. Lett. **93** (16), 165002 (2004).

[31] T. Ido *et al.*, Nucl. Fusion **46**, 512 (2006).

[32] K. Itoh *et al.*, Plasma Fusion Res. **1**, 037 (2006).

[33] M. Sasaki, K. Itoh, A. Ejiri and Y. Takase, Contrib. Plasma Phys. **48**, 68 (2007).

[34] S.-I. Itoh, K. Itoh, M. Sasaki, A. Fujisawa, T. Ido and Y. Nagashima, Plasma Phys. Control. Fusion **49**, No.8, L7 (2007).

[35] Y. Nagashima *et al.*, Phys. Rev. Lett. **95**, 095002 (2005).

[36] Y. Nagashima *et al.*, Plasma Phys. Control. Fusion **48**, S1 (2006).

[37] Y. Nagashima, K. Itoh, A. Fujisawa, K. Shinohara, S.-I. Itoh *et al.*, Plasma Phys. Control. Fusion **51**, 065019 (2009).

[38] Y. Nagashima, K. Hoshino, K. Shinohara, K. Uehara, Y. Kusama, K. Nagaoka, A. Fujisawa, K. Ida, Y. Yoshimura, S. Okamura, K. Matsuoka, A. Ejiri, Y. Takase, K. Itoh, M. Yagi, S.-I. Itoh, JFT-2M group and CHS group, Plasma Fusion Res. **1**, 041 (2006).

[39] Y. Nagashima, K. Itoh, S.-I. Itoh, M. Yagi, A. Fujisawa, K. Hoshino, K. Shinohara, K. Uehara, Y. Kusama, A. Ejiri and Y. Takase, Rev. Sci. Instrum. **77**, No.4, 045110 (2006).

[40] Y. Nagashima, K. Itoh, S.-I. Itoh, K. Hoshino, A. Fujisawa, A. Ejiri, Y. Takase, M. Yagi, K. Shinohara, K. Uehara, Y. Kusama and JFT-2M group, Plasma Phys. Control. Fusion **48**, A377 (2006).

[41] Y. Nagashima, K. Itoh, S.-I. Itoh, A. Fujisawa, M. Yagi, K. Hoshino, K. Shinohara, A. Ejiri, Y. Takase, T. Ido, K. Uehara, Y. Miura and JFT-2M group, Plasma Phys. Control. Fusion **49**, 1611 (2007).

[42] K. Itoh *et al.*, Phys. Plasmas **12**, 102301 (2005).

[43] T. Ido *et al.*, Plasma Phys. Control. Fusion **48**, S41 (2006).

[44] G.R. Tynan *et al.*, Plasma Phys. Control. Fusion **48**, S51 (2006).

[45] A. Fujisawa *et al.*, Plasma Phys. Control. Fusion **48**, S205 (2006).

[46] A. Fujisawa, A. Shimizu, H. Nakano, S. Ohsima, K. Itoh, H. Iguchi, K. Matsuoka, S. Okamura1, S.-I. Itoh and P.H. Diamond, Plasma Phys. Control. Fusion **48**, A365 (2006).

[47] A. Fujisawa, A. Shimizu, H. Nakano, S. Ohshima, K. Itoh, Y. Nagashima, S.-I. Itoh, H. Iguchi, Y. Yoshimura, T. Minami, K. Nagaoka, C. Takahashi, M. Kojima, S. Nishimura, M. Isobe, C. Suzuki, T. Akiyama, T. Ido, K. Matsuoka, S. Okamura and P.H. Diamond, Plasma Phys. Control. Fusion **49**, No.3, 211 (2007).

[48] A. Fujisawa, A. Shimizu, H. Nakano, S. Ohshima, K. Itoh, Y. Nagashima, S.-I. Itoh, H. Iguchi, Y. Yoshimura, T. Minami, K. Nagaoka, C. Takahashi, M. Kojima, S. Nishimura, M. Isobe, C. Suzuki, T. Akiyama, T. Ido, K. Matsuoka, S. Okamura and P.H. Diamond, J. Phys. Soc. Jpn. **76**, 033501 (2007).

[49] A. Fujisawa, Plasma Phys. Control. Fusion **45**, R1 (2003).

[50] K. Itoh, S. Toda, A. Fujisawa, S.-I. Itoh M. Yagi, A. Fukuyama, P.H. Diamond and K. Ida, Phys. Plasmas **14**, No.2, 020702 (2007).

[51] A. Yoshizawa, S.-I. Itoh, K. Itoh and N. Yokoi, Plasma Phys. Control. Fusion **46**, R25 (2004).

[52] A. Fujisawa, K. Itoh, A. Shimizu, H. Nakano, S. Ohshima, H. Iguchi, K. Matsuoka, S. Okamura, T. Minami, Y. Yoshimura, K. Nagaoka, K. Ida, K. Toi, C. Takahashi, M. Kojima, S. Nishimura, M. Isobe, C. Suzuki, T. Akiyama, Y. Nagashima, S.-I. Itoh and P.H. Diamond, Phys. Rev. Lett. **98**, 165001 (2007).

[53] A. Fujisawa, K. Itoh, A. Shimizu, H. Nakano, S. Ohshima, H. Iguchi, K. Matsuoka, S. Okamura, T. Minami, Y. Yoshimura, K. Nagaoka, K. Ida, K. Toi, C. Takahashi, M. Kojima, S. Nishimura, M. Isobe, C. Suzuki, T. Akiyama, T. Ido, Y. Nagashima, S.-I. Itoh and P.H. Diamond, Phys. Plasmas **15**, 055906 (2008).

[54] A. Fujisawa, A. Shimizu, H. Nakano and S. Ohshima, Plasma Phys. Control. Fusion **49**, 845 (2007).

[55] A. Fujisawa *et al.*, ICPP2008, paper FB.O1-X-2.

[56] T. Yamada, S.-I. Itoh, T. Maruta, N. Kasuya, S. Shinohara, Y. Nagashima, M. Yagi, K. Terasaka, S. Inagaki, Y. Kawai, M. Fukao, A. Fujisawa and K. Itoh, Plasma Fusion Res. **3**, 044 (2008).

[57] N. Kasuya *et al.*, J. Phys. Soc. Jpn. **76**, 044501 (2007).

[58] T. Yamada, S.-I. Itoh, T. Maruta, N. Kasuya, Y. Nagashima, S. Shinohara, K. Terasaka, M. Yagi, S. Inagaki, Y. Kawai, A. Fujisawa and K. Itoh, Nature Phys. **4**, 721 (2008).

[59] K. Terasaka *et al.*, Plasma Fusion Res. **2**, 031 (2007).

[60] T. Yamada *et al.*, Rev. Sci. Instrum. **78**, 123501 (2007).

[61] T. Yamada *et al.*, Plasma Fusion Res. **2**, 051 (2007).

[62] Y. Saitou, A. Yonesu, S. Shinohara, M.V. Ignatenko, N. Kasuya, M. Kawaguchi, K. Terasaka, T. Nishijima, Y. Nagashima, Y. Kawai, M. Yagi, S.-I. Itoh, M. Azumi and K. Itoh, Phys. Plasmas **14**, 702301 (2007).

[63] M. Ignatenko, M. Azumi, M. Yagi, S. Shinohara, S.-I. Itoh and K. Itoh, Jpn. J. App. Phys. **46**, Part1 No.4A, 1680 (2007).

[64] T. Yamada *et al.*, to be published in J. Plasma Fusion Res. Series **8**, 87 (2009).

[65] S.-I. Itoh and K. Itoh, Plasma Phys. Control. Fusion **50**, No.5, 055002 (2008).

[66] N. Kasuya, M. Yagi, K. Itoh and S.-I. Itoh, Phys. Plasmas **15**, 052302 (2008).

[67] S. Inagaki *et al.*, ICPP2008 paper FB.P1-019.

[68] Y. Nagashima, S.-I. Itoh, S. Shinohara, M. Fukao, A. Fujisawa *et al.*, J. Phys. Soc. Jpn. **77**, 114501 (2008).

[69] Y. Nagashima, S.-I. Itoh, S. Shinohara, M. Fukao, A. Fujisawa *et al.*, Phys. Plasmas **16**, 020706 (2009).

[70] Y. Nagashima, to be published in J. Plasma Fusion Res. Series **8**, 50 (2009).

[71] N. Kasuya *et al.*, to be published in J. Plasma Fusion Res. Series **8**, 77 (2009).

[72] It is noted that the quasi-linear theory may provide, under some circumstances, a good approximation (e.g., S. Hamaguchi *et al.* Phys. Fluids **2** 1833 (1990), or some example in [27]). The essential issue is that the quasi-linear theory has limitation in judging whether it is sufficiently

correct or not: This conclusion must be drawn by the non-linear theory in which dynamics of multiple-scale structures are incorporated.

[73] Sanae-I. Itoh, Kimitaka Itoh, A. Yoshizawa and N. Yokoi, Astrophys. J. **618**, 1044 (2005).

[74] S.-I. Itoh, K. Itoh, P.H. Diamond and A. Yoshizawa, Publ. Astron. Soc. Jpn. **58**, No.3 (June), 605 (2006).

[75] *Solar tachocline* (Cambridge Univ. Press 2007).

[76] K. Ida, S. Inagaki, R. Sakamoto, K. Tanaka, H. Funaba, Y. Takeiri, K. Ikeda, C. Michel, T. Tokuzawa, H. Yamada, Y. Nagayama, K. Itoh O. Kaneko, A. Komori, O. Motojima and the LHD experimental group, Phys. Rev. Lett. **96**, 125006 (2006).

[77] S. Inagaki, N. Tamura, T. Tokuzawa, S.V. Neudatchin, K. Itoh, K. Ida, M. Yakovlev, K. Tanaka, Y. Nagayama, K. Kawahata, S. Sudo and LHD experimental group, Plasma Phys. Control. Fusion **48**, A251 (2006).

[78] S. Inagaki, H. Takenaga, K. Ida, A. Isayama, N. Tamura, T. Takizuka, T. Shimozuma, Y. Kamada, S. Kubo, Y. Miura, Y. Nagayama, K. Kawahata, S. Sudo, K. Ohkubo, LHD Experimental group and the JT-60 Team, Nucl. Fusion **46**, No.1, 133 (2006).

[79] N. Tamura, S. Inagaki, K. Tanaka, C. Michal, T. Tokuzawa, T. Shimozuma, S. Kubo, R. Sakamoto, K. Ida, K. Itoh, D. Kalinina, S. Sudo, Y. Nagayama, K. Kawahata, A. Komori and the LHD Experimental group, Nucl. Fusion **47**, No.5, 449 (2007).

[80] S. Inagaki, N. Tamura, Y. Nagashima, T. Tokuzawa, T. Yamada, K. Ida, T. Maruta, S. Kubo, K. Terasaka, T. Shimozuma, Y. Nagayama, K. Kawahata, A. Komori, S. Shinohara, A. Fujisawa, M. Yagi, Y. Kawai, S.-I. Itoh, K. Itoh and the LHD experimental group, Plasma Fusion Res. **3**, S1006 (2008).

[81] K. Ida, Y. Sakamoto, H. Takenaga, N. Oyama, K. Itoh, M. Yoshinuma, S. Inagaki, T. Kobuchi, A. Isayama, T. Suzuki, T. Fujita, G. Matsunaga, Y. Koide, M. Yoshida, S. Ide, Y. Kamada and JT-60 team, Phys. Rev. Lett. **101**, 055003 (2008).

[82] K. Itoh *et al.*, ICPP2008, paper FB.P1-023, to be published in J. Plasma Fusion Res. Series Vol.8 (2009).

[83] K. Kamataki, Y. Nagashima, S. Shinohara, Y. Kawai, M. Yagi, K. Itoh and S.-I. Itoh, J. Phys. Soc. Jpn. **76**, No. 5, 054501 (2007).

[84] K. Kamataki, S.-I. Itoh, Y. Nagashima, S. Inagaki, S. Shinohara, M. Yagi, T. Yamada, Y. Kawai, A. Fujisawa and K. Itoh, Plasma Phys. Control. Fusion **50**, 035011 (2008).

[85] H. Tsuchiya, S.-I. Itoh, A. Fujisawa, K. Kamataki, S. Shinohara, M. Yagi, Y. Kawai, A. Komori and K. Itoh, Plasma Phys. Control. Fusion **50**, 055005 (2008).

[86] N. Kasuya and K. Itoh, Phys. Rev. Lett. **94**, 195002 (2005).

[87] N. Kasuya, K. Itoh and Y. Takase, J. Plasma Fusion Res. **81**, 553 (2005).

[88] N. Kasuya and K. Itoh, Phys. Plasmas **12**, No.9, 090905 (2005).

[89] N. Kasuya and K. Itoh, Plasma Phys. Control. Fusion **48**, A319 (2006).

[90] N. Kasuya and K. Itoh, Nucl. Fusion **48**, 035003 (2008).

[91] M. Yagi *et al.*, ICPP2008, paper FB.P1-025, to be published in J. Plasma Fusion Res. Series Vol.8 (2009).